

Numerical Investigation of the Structure of Fracture Network Impact on the Fluid Flow through a Poroelastic Medium

D. Yu. Legostaev^{a,*} and S. P. Rodionov^{a,**}

^a*Tyumen Branch of the Khristianovich Institute of Theoretical and Applied Mechanics,
Siberian Branch of the Russian Academy of Sciences, Tyumen, Russia*

**e-mail: legostaevdy@yandex.ru*

***e-mail: rodionovsp@bk.ru*

Received August 5, 2022; revised November 12, 2022; accepted December 21, 2022

Abstract—Two-dimensional single-phase flow of a weakly compressible fluid through a deformable fractured-porous medium is considered. A poroelastic model is used for coupled simulation of the fluid flow and the related changes in the stress state of the medium. Fracture network is simulated using the discrete fracture model. The fractures in the region under consideration have random location and orientations, and the fracture length distribution follows a power law. The dependence of the hydraulic properties of fractured porous media on its stress-strain state and the structure of the fracture network is studied. Numerical study was performed for various realizations of fracture network obtained using multiple random generation. It is found that the permeability of the fractured porous medium is determined mainly by the structure of the fracture system characterized by the percolation parameter. According to the simulations results, hydraulic properties are significantly affected by the stress-strain state only for connected fracture systems. An approximation is proposed to define the dependence of the equivalent permeability of a fractured-porous medium on the following parameters: the connectivity of the fracture system, the stress-strain state of the medium, and fracture properties such as stiffness and aperture.

Keywords: fractured-porous medium, absolute permeability, poroelasticity, single-phase flow through a porous medium, discrete fracture model, stress-strain state, percolation

DOI: 10.1134/S001546282360027X

The study of liquid and gas flows through rocks and other porous media is important in various applications [1–3]. The rocks can contain fractures, both natural and artificial, obtained, for example, during the reservoir hydraulic fracturing [4, 5]. At the same time, fractures significantly affect fluid flow through porous reservoirs [6, 7]. Having high conductivity, the fractures can serve as the main channels in the flow of liquids and gases. For example, in the development of oil fields, the presence of fracture system can lead to early breakthroughs of the injected water to production wells and decrease of oil displacement efficiency. In this connection, the presence of fractures must be taken into account when planning the placement and performance of wells [8].

An important issue in simulation of the processes of fluid flow through fractured media is the choice of approach to fracture simulation, which should take into account the structure and properties of the fracture system. The most universal approach is the discrete-fracture model [9, 10], which makes it possible to take into account the location, the orientation, the size, and the physical properties of each fracture in the system. This approach has no restrictions on the geometric structure of the fracture system, but its applicability is limited by high computational complexity. In addition, for highly fractured media it is not possible to describe the geometric characteristics of each individual fracture. In this case, the dual porosity/dual permeability model [11, 12] is used to simulate fracture network. Within the framework of this model, the rock matrix and the fracture system are represented as continuous media with effective properties. The hydraulic properties of fractured rocks strongly depend on the stress-strain state of the medium [13]. The model of the poroelastic medium is often used to describe the coupled processes of flow through porous media and the related changes in the stress-strain state of the medium [10, 14, 15].

A significant degree of uncertainty in the parameters of the fracture system is the key factor in modeling of fractured media. Since the true location of all fractures in the reservoir is not reliably known, it becomes necessary to use a probabilistic description of the fracture system, which involves using the distribution

laws for fractures in length, angle, space, and aperture [16, 17]. The power law [18] is most widely used to describe the fracture distribution over the lengths. This law makes it possible to describe the different scales inherent in the system of fractures. The permeability of fractured media significantly depends on the parameters of the fracture system [19, 20], the most significant of these parameters are the fracture length and the fracture concentration in the area under consideration [21].

The methods of theory of percolation [22–25] along with the methods of continuum mechanics are widely used to analyze the effect of fracture system on the rock permeability. The use of the former makes it possible to estimate the connectivity and conductivity of a fracture system based on its geometric characteristics. In this case, the connectivity of the opposite boundaries of the area under consideration through the system of fractures, characterized by the percolation parameter, significantly affects the permeability of the medium.

The aim of this work is to study the dependence of the permeability of fractured-porous media as a function of their stress-strain state and the structure of the fracture system. The equivalent permeability of a deformable fractured-porous medium are determined from the results of direct numerical simulation of the single-phase flow in a two-dimensional region. The study is carried out for different realizations of fracture systems obtained by multiple random generation. The influence of the density of a system of fractures and the percolation parameter on the equivalent permeability of the medium is considered. The dependence of the equivalent permeability of the medium on its stress-strain state is studied at various pressures of fluid injection into the region considered. A form of approximating function that takes into account the dependence of the permeability of the fractured-porous medium on the main parameters of the problem under consideration is proposed.

1. MATHEMATICAL MODEL

We will consider a single-phase two-dimensional flow of a weakly compressible fluid through a deformable fractured-porous medium. We will use a mathematical model of the poroelastic medium to describe the processes of flow through a fractured porous medium. The model includes equations for the fluid pressure in the matrix-fracture system and equations for the displacement of the rock skeleton, which take into account the deformation properties of fractures.

1.1. Fluid Flow through a Fractured-Porous Medium

The equation of fluid flow in the porous space of the deformable skeleton of a rock can be written in the form [15]:

$$\frac{1}{M_m} \frac{\partial P_m}{\partial t} + b_m \frac{\partial}{\partial t} (\nabla \cdot \mathbf{u}) = -\nabla \cdot \mathbf{v}_m,$$

where P_m is the fluid pressure in the porous space, $M_m = C_l \phi_m + \frac{b_m - \phi_m}{K_s}$ is the Biot modulus of the porous medium, C_l is the compressibility of fluid, ϕ_m is the porosity of the rock matrix, b_m is the Biot coefficient of the rock matrix, K_s is the volume modulus of the rock grains, \mathbf{u} is the vector of displacements of the rock skeleton, and \mathbf{v}_m is the fluid flow velocity in the porous space.

The fluid flow velocity through the porous medium can be determined from Darcy’s equation

$$\mathbf{v}_m = -\frac{k_m}{\mu_l} \nabla P_m,$$

where k_m is the absolute permeability of the porous medium and μ_l is the fluid viscosity.

A fracture represents two surfaces Γ_+ and Γ_- in mechanical contact, their roughness does not allow them to close completely. The longitudinal dimensions of the fracture are significantly greater than its transverse dimensions. This makes it possible to consider fractures in the two-dimensional case as one-dimensional objects. When considering the processes of flow through a porous medium, the fracture is modeled as a narrow gap surrounded by a rock matrix. The equation for the fluid pressure in the fracture, which takes into account the poroelastic effects, takes the form [13]:

$$\frac{\delta}{M_f} \frac{\partial P_f}{\partial t} + b_f \frac{\partial u_n}{\partial t} = -\frac{\partial q_f}{\partial x_f} - v_+ - v_-,$$

where δ is the fracture aperture, P_f is the fluid pressure in the fracture, $M_f = C_l \phi_f + \frac{b_f - \phi_f}{K_s}$ is the Biot modulus of the fracture, ϕ_f is the fracture porosity, b_f is the Biot coefficient of the fracture, x_f is the coordinate along the fracture, q_f is the flow flux along the fracture, and v_{\pm} is the fluid flow velocity along the normal to the fracture boundaries.

The fluid flow in a fracture is considered as a motion between two parallel planes located at a distance δ from each other. The linear flow rate through the fracture in accordance with the cubic law [26] has the form:

$$q_f = -\frac{\delta^3}{12\mu_l} \frac{\partial P_f}{\partial x_f}.$$

By analogy with Darcy's law, the expression for the absolute permeability of a fracture can be written as follows:

$$k_f = \frac{\delta^2}{12} = \frac{(\delta_0 + \Delta\delta)^2}{12},$$

where δ_0 is the characteristic fracture aperture and $\Delta\delta$ is a change in the aperture.

The pressure and the flow flux continuity conditions must be satisfied on the fracture boundaries Γ_{\pm} . In this case, the fluid flow velocity v_{\pm} along the normal to the matrix-fracture boundary Γ_{\pm} is proportional to the pressure gradient and can be determined as follows:

$$v_{\pm} = -\frac{k_m}{\mu_l} \frac{\partial P_m}{\partial \mathbf{n}_{\pm}},$$

where \mathbf{n}_{\pm} is the normal vector to the fracture boundaries.

When considering a system of fractures, two fractures either do not intersect or have one common point. In this case, at the point of intersection of fractures, the conditions for the continuity of pressure and flows must also be satisfied.

1.2. Stress-Strain State of a Fractured-Porous Medium.

At every instant of time the fractured-porous medium is in the state of mechanical equilibrium. For the poroelastic medium the momentum conservation law in the quasi-stationary approximation without taking into account body forces takes the form [15]:

$$\nabla \cdot \boldsymbol{\sigma} = \nabla \cdot (\boldsymbol{\sigma}' - b_m \nabla P_m I) = 0, \quad (1.1)$$

where $\boldsymbol{\sigma}$ is the total stress tensor, $\boldsymbol{\sigma}'$ is the effective stress tensor, and I is the unit matrix.

For an isotropic poroelastic medium in the case of small deformations, using Hooke's law, equation (1.1) can be written in term of the displacement vector of the rock skeleton as follows:

$$\nabla \cdot [\mu \nabla \mathbf{u} + \mu (\nabla \mathbf{u})^T + \lambda I \text{tr}(\nabla \mathbf{u})] - b_m \nabla P_m = 0,$$

where λ and μ are the Lamé coefficients.

In simulating the stress-strain state, the fractures are considered as inclusions in the rock skeleton, which have their own deformation properties. In accordance with the condition of mechanical equilibrium (1.1), the stresses acting on the fracture boundaries must satisfy the condition

$$\boldsymbol{\sigma}_+ \cdot \mathbf{n}_+ = -\boldsymbol{\sigma}_- \cdot \mathbf{n}_-,$$

where $\boldsymbol{\sigma}_+$ and $\boldsymbol{\sigma}_-$ are the total stresses acting on opposite sides of the fracture.

The expression for the effective stresses arising in the fracture can be represented in the form:

$$\boldsymbol{\sigma}'_n = \boldsymbol{\sigma}_n + b_f P_f, \quad \boldsymbol{\sigma}'_s = \boldsymbol{\sigma}_s, \quad (1.2)$$

where $\boldsymbol{\sigma}_n$ and $\boldsymbol{\sigma}_s$ are the total normal and shear stresses and $\boldsymbol{\sigma}'_n$ and $\boldsymbol{\sigma}'_s$ are the effective normal and shear stress. From (1.2) it can be seen that the fluid pressure in the fracture does not affect the shear stress component.

The normal and shear stresses acting on the fracture are connected with the relative displacements of its boundaries by the following linear relations:

$$\sigma'_n = k_n u_n, \quad \sigma'_s = k_s u_s, \tag{1.3}$$

where u_n and u_s are the relative normal and shear displacements of the fracture faces.

The fracture aperture δ can be expressed in terms of the relative normal displacement of its edges:

$$\delta = \delta_0 + \Delta\delta = \delta_0 + u_n.$$

Thus, the above equations of single-phase flow through a deformable fractured-porous medium form a closed system, which must be supplemented with initial and boundary conditions.

2. FORMULATION OF THE PROBLEM

We will consider a fluid-saturated fractured-porous medium located in a square region $\Omega = \{0 \leq x \leq L; 0 \leq y \leq L\}$ with the left-hand, right-hand, bottom, and top boundaries $\Gamma_l = \{x = 0; 0 \leq y \leq L\}$, $\Gamma_r = \{x = L; 0 \leq y \leq L\}$, $\Gamma_b = \{0 \leq x \leq L; y = 0\}$, and $\Gamma_t = \{0 \leq x \leq L; y = L\}$, respectively.

2.1. Boundary and Initial Conditions

We will consider the flows through the porous medium in the horizontal direction caused by a constant pressure difference between the left- and right-hand boundaries of the computational domain $P_{in} - P_{out} = \Delta P$. The no-flow condition is imposed on the upper and lower boundaries of the computational domain. Thus, the boundary conditions for the pressure have the form:

$$P|_{\Gamma_r} = P_{out}, \quad \frac{\partial P}{\partial \mathbf{n}}|_{\Gamma_t} = 0, \quad P|_{\Gamma_l} = P_{in}, \quad \frac{\partial P}{\partial \mathbf{n}}|_{\Gamma_b} = 0.$$

The fractured-porous medium is under the impact of the total compressive stresses that act perpendicular to the boundaries of the region. To take into account the influence of rocks adjacent to the computational area, the boundary conditions of the “absolutely rigid plate” are used [27]. This leads to the following boundary conditions:

$$\int_{\Gamma_r} \sigma dy = \sigma_b L, \quad \int_{\Gamma_l} \sigma dx = \sigma_b L, \quad \mathbf{u}_n|_{\Gamma_l} = 0, \quad \frac{\partial \mathbf{u}_\tau}{\partial \mathbf{n}}|_{\Gamma_l} = 0, \quad \mathbf{u}_n|_{\Gamma_b} = 0, \quad \frac{\partial \mathbf{u}_\tau}{\partial \mathbf{n}}|_{\Gamma_b} = 0,$$

where \mathbf{u}_n and \mathbf{u}_τ are the normal and shear components of the displacement vector.

At the initial instant, the fluid pressures in the pore space and fractures are identical $P_m|_{\Omega} = P_f|_{\Omega} = P_i$, while the displacement field \mathbf{u}_i and the fracture aperture δ_i are determined from the solution of the formulated problem for the unperturbed pressure fields at $P_{in} = P_{out} = P_i$. All values of the pressures and stresses are reckoned from the initial pressure P_i .

2.2. Fracture Network

In the area under consideration, there is a fracture system, consisting of fractures with random location and orientations. The fracture distribution in lengths follows the power law [18]

$$n(l) = Al^{-a}, \tag{2.1}$$

where $l \in [l_{min}, l_{max}]$ is the fracture length, $n(l)dl$ is the number of fractures with the size l falling in the interval $[l, l + dl]$, a is the exponent, and A is a normalization constant.

The fracture system can be characterized by the density γ and the percolation parameter p , the expressions for which are as follows [22]:

$$\gamma = \frac{1}{L^2} \int_{l_{min}}^{l_{max}} n(l)l' dl,$$

and

$$p = \frac{1}{L^2} \int_{l_{\min}}^{l_{\max}} n(l)l^2 dl,$$

where l is the length of the fracture included in the region under consideration. The percolation parameter p characterizes the degree of connectivity of the fracture system. For $p > p_c$, where p_c is the percolation threshold, the fractures statistically connect opposite boundaries of the region under consideration.

3. TECHNIQUE OF NUMERICAL SOLUTION

The above system of equations was solved numerically using the control volume method [28]. The coupled solution of the equations of poroelasticity for the fractured medium was implemented using “with the fixed-stress” sequential scheme [29], which is unconditionally stable. To take into account the location of fractures within the computational domain, unstructured computational grids were used. The grids were constructed using the open software Gmsh [30]. Numerical calculations were carried out using the original author’s program module [31].

Despite the fact that the discrete fracture model allows the most accurate description of the fractured medium, it is complicated because of high cost associated with time-consuming fine-mesh computations. Realization of the fracture system obtained by random generation may have a geometry that requires an excessive refinement of the computational grid [32]. In this connection, some restrictions on the process of generating a fracture system were imposed to avoid such refinement: the minimum distance between non-intersecting fractures d_{\min} , the minimum distance between fracture intersection points d_{\min} , and the minimum fracture intersection angle θ_{\min} .

4. RESULTS AND DISCUSSION

An important issue in studying the effect of fracture network on the hydraulic properties of rocks is the investigation of the dependence of the equivalent permeability of the medium on the structure of the fracture system. The equivalent absolute permeability of a fractured-porous medium k_{eq} can be found from Darcy’s equation for a given pressure drop between the boundaries of the computational domain ΔP and a known fluid flow rate q in the steady flow:

$$q = -\frac{k_{\text{eq}} \Delta P}{\mu_l L},$$

hence

$$k_{\text{eq}} = -\frac{q\mu_l L}{\Delta P}.$$

In the present study, the dependence of the equivalent permeability of a fractured-porous medium on its stress-strain state and parameters characterizing the structure of the fracture system is investigated. For this purpose, multiple random generation of the fracture systems was carried out. For each of the realization, the problem of single-phase fluid flow through a deformable fractured-porous medium was solved numerically. The equivalent permeability was calculated on the basis of the fluid flow rates obtained from the numerical solution on opposite boundaries of the computational domain. The solution for the stationary flow regime was obtained by the relaxation method. The size of the time step and the characteristic dimensions of the computational nodes are taken in such a way that their further reduction has no significant effect on the calculation results.

In all calculations, the following values of the parameters of the rock and the saturating fluid were used: the matrix porosity $\phi_m = 0.14$, the fracture porosity $\phi_f = 1.0$, the matrix permeability $k_m = 1 \times 10^{-15} \text{ m}^2$, the fracture aperture in the undeformed state $\delta_0 = 5 \times 10^{-4} \text{ m}$, Young’s modulus $E = 2 \times 10^4 \text{ MPa}$, Poisson’s ratio $\nu = 0.2$, the bulk modulus of grain material $K_s = 2.7 \times 10^5 \text{ MPa}$, the normal fracture stiffness $k_n = 2 \times 10^5 \text{ MPa/m}$, the fracture shear stiffness $k_s = 1 \times 10^5 \text{ MPa/m}$, the matrix Biot coefficient $b_m = 1.0$, the fracture Biot coefficient $b_f = 1.0$, the fluid compressibility coefficient $C_l = 3.7 \times 10^{-4} \text{ MPa}^{-1}$, and the fluid viscosity $\mu_l = 1.0 \text{ mPa s}$.

The fracture permeability k_f depends on the fracture aperture, determined by the stress-strain state of the medium. Change in the permeability of a porous medium caused by change in the stress-strain state can be neglected in comparison with the change in the fracture permeability. For fractures of all sizes, the same aperture δ_0 was used. The ratio of the fracture and porous matrix permeabilities at $\delta = \delta_0$ is equal to $k_f/k_m \approx 10^4$. The size of the side of computational domain L was set equal to 250 m, which corresponds to the characteristic distance between wells in the development of oil reservoirs.

4.1. Variants of the Fracture System

To study the effect of fracture system on the hydraulic properties of the medium, fracture systems with various exponents a in the power law (2.1) and number of fractures in the system n_f are considered. The exponent in the distribution law took the values $a = 1.5, 2.0, 2.5, 3.0,$ and 3.5 the number of fractures in the system was equal to $n_f = 50, 100, 150,$ and 200 . For each pair of values of the parameters a and n_f , 40 implementations of the fracture systems were created. Thus, in total, $N = 5 \times 4 \times 40 = 800$ realizations of the fracture systems were considered in the work. For all cases, the values of $l_{\max} = 2L = 500$ m and $l_{\min} = 0.06L = 15$ m were taken. When generating the fracture systems, we took $d_{\min} = 5$ m and $\theta_{\min} = 20^\circ$. The density and percolation parameter for all realizations of the fracture systems belonged to the following intervals: $\gamma \in [0.016; 0.202]$ and $p \in [0.4; 26.2]$.

In Fig. 1 we have reproduced some examples of the generated fracture systems for each of the pairs (n_f, a) and the corresponding values of γ and p . It can be seen that, as a decreases, the characteristic length of fractures increases and their connectivity increases. Thus, at $a = 3.5$, fractures of small length isolated from each other predominate in the region. At $a = 1.5$, most of the fractures are included in one cluster connecting the opposite boundaries of the computational domain.

By percolation we mean the connection of opposite boundaries of the computational domain by a fracture system. In this case, there is at least one path along the fractures from one boundary to another. A set of fractures connecting the boundaries forms a percolation cluster. For each variant of the fracture system, the presence of a connection between the opposite boundaries of the region in the horizontal direction was studied. For the considered set of fracture systems, in 357 cases percolation of the computational domain takes place, and in 443 cases the opposite boundaries are disconnected. In Fig. 2 we have reproduced the dependence of the probability of percolation of the computational domain on the percolation parameter, which is approximated by a function of the following form:

$$S(p) = \frac{1}{1 + e^{-\varepsilon(p-p_c)}}, \tag{4.1}$$

where p_c is the percolation threshold and ε determines the width of the “zone.”

The mean absolute error $mae = \frac{1}{n} \sum_{i=1}^n |\hat{y}_i - y_i|$, where \hat{y}_i is the result of the approximation and y_i is the true value, were used to estimate the approximation quality. The obtained value $mae = 0.1$ testifies to the satisfactory quality of the approximation. The percolation threshold p_c is taken to be the value at which the probability of percolation of the computational domain is $S(p) = 0.5$. As a result of approximation from (4.1) the value $p_c = 4.8$ was obtained. Depending on the probability of percolation, each system of fractures can be conditionally assigned to one of the three groups divided in Fig. 2 by vertical lines. The systems of weakly connected fractures include realizations for which the probability of appearance of a percolation cluster is $S(p) \leq 0.01$, which corresponds to the percolation parameter $p \leq 1.7$. The realizations of fracture systems for which $S(p) \geq 0.99$ are classified as strongly connected: $p \geq 7.9$. The fracture systems from the interval $1.7 < p < 7.9$ are assigned to the “transition zone,” in which the appearance of a percolation cluster is random.

4.2. Effect of the Fractured Medium Parameters on the Equivalent Permeability

First, we will consider the influence of the structure of a fractured medium on its equivalent permeability at a fixed fracture aperture δ_i , which corresponds to the initial stress-strain state of the medium at an external load $\sigma_b = 15$ MPa. In this case, an arbitrary pressure drop can be taken to determine the equivalent permeability of the medium, in our calculations we took $\Delta P = 5$ MPa.

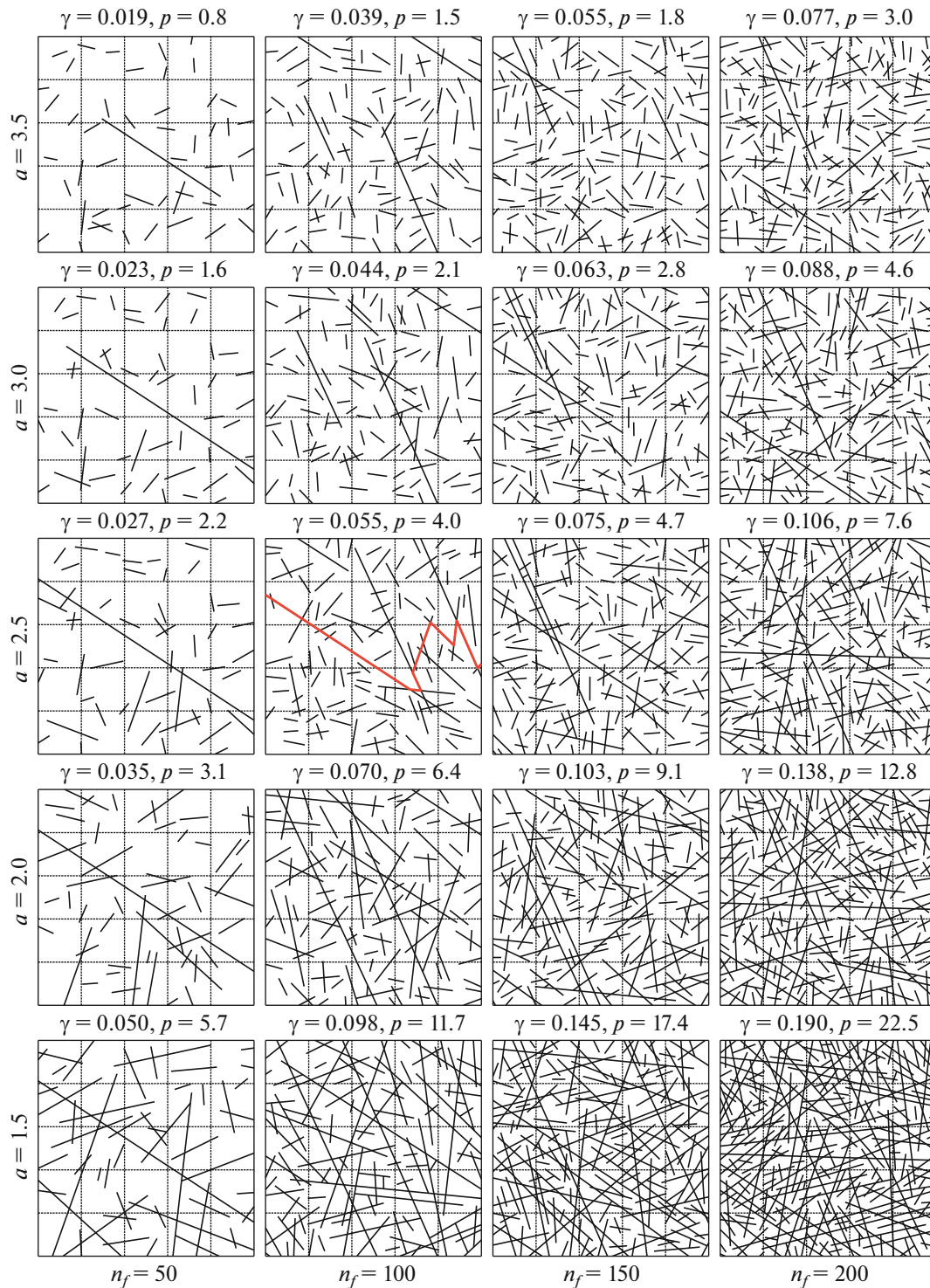


Fig. 1. Examples of realization of generated fracture systems with various values of the power law exponent a of the fracture length distribution (rows) and the number of fractures in the system n_f (columns). For each system of fractures, the values of the density of fracture system γ and the percolation parameter p are given.

In Fig. 3 have plotted the graphs of the quantity k_{eq}/k_m as a function of γ in the semilogarithmic coordinates for various values of a . Filled markers correspond to the highly permeable media with fractures forming a percolation cluster. At the weak connectivity of fractures and the absence of percolation cluster,

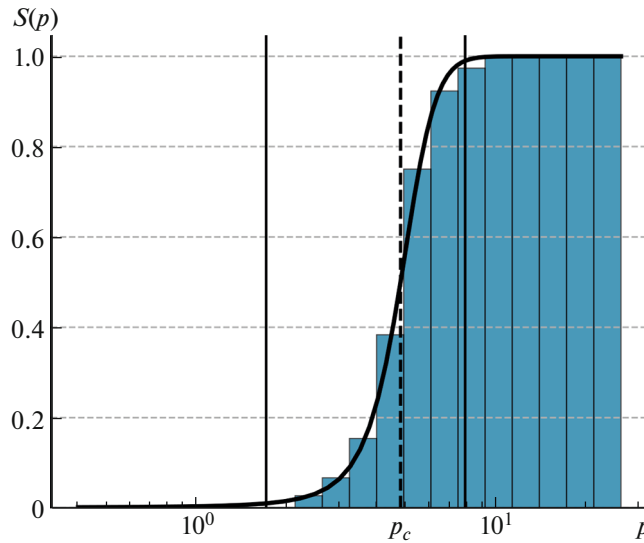


Fig. 2. Probability of the connection of opposite boundaries of the computational domain by a fracture system as a function of the percolation parameter p . The threshold value of the percolation parameter $p_c = 4.8$.

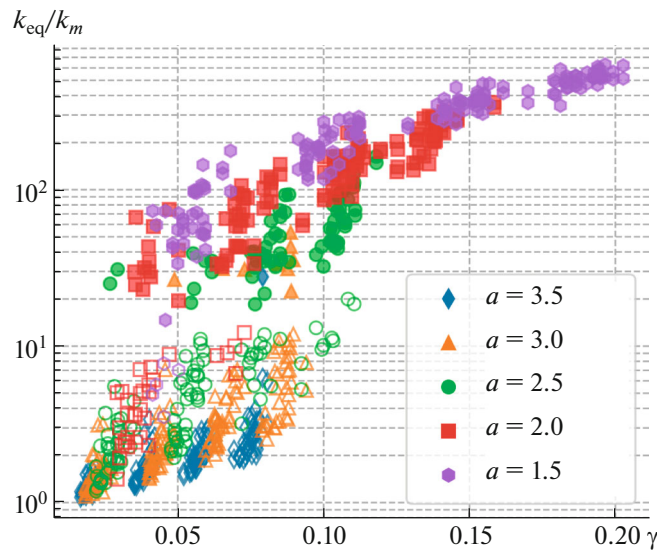


Fig. 3. Ratio k_{eq}/k_m as a function of the density of the fracture system γ at various exponents a . Filled markers correspond to the case of percolation of the computational domain and hollow markers correspond to the absence of the percolation cluster.

a low equivalent permeability of the medium is observed; these realizations are indicated by hollow markers. Thus, for the permeabilities $k_f \gg k_m$ under consideration, the presence of a percolation cluster has the decisive effect on the equivalent permeability of the fractured medium. It can be seen that the calculated values can be divided into two “clouds” of points. The region between the “clouds,” in which there are no calculated points, corresponds to the percolation threshold, and its presence is attributable to the use of a constraint on the minimum distance between non-intersecting fractures d_{min} in the algorithm of fracture system generation.

To analyze the behavior of the equivalent permeability of the fractured porous medium near the percolation threshold, we consider an idealized fractured medium consisting of a set of parallel fractures [33]. The fractures of the identical length l_f are located at the same distance from each other and oriented along

the flow. In this case, if the fracture length is greater than the size of the computational domain $l_{\parallel} \geq L$, then the permeability of the medium can be determined as the arithmetic mean of the permeabilities of the porous medium and fractures:

$$k_{\parallel}^I = k_m \left(1 - \frac{\delta n_f}{L} \right) + k_f \frac{\delta n_f}{L}. \quad (4.2)$$

Otherwise, if the fracture length in the system is less than the dimensions of the computational domain $l_{\parallel} < L$, then the permeability is estimated using the harmonic weighted mean permeability of the model fractured-porous medium (4.2) and the rock matrix:

$$k_{\parallel}^{II} = \frac{L k_m k_{\parallel}^I}{l_{\parallel} k_m + (L - l_{\parallel}) k_{\parallel}^I}. \quad (4.3)$$

The ratio l_{\parallel}/L has the meaning of the proportion of the computational area occupied by fractures. As follows from (4.3), at $k_m \ll k_f$ the rock matrix restricts the value of fluid flow rate. At the same time, as $l_{\parallel} \rightarrow L$, the permeability of the computational domain rapidly increases to k_{\parallel}^I , which is mainly determined by k_f . Thus, the behavior of the equivalent permeability near the percolation threshold is continuous.

From Fig. 3 it also follows that significantly different values of the equivalent permeability can be realized at close values of the density of the fracture system. As an example, we will consider the equivalent permeabilities for the fracture systems shown in Fig. 1. For example, for the ($a = 1.5$, $n_f = 50$), ($a = 2.5$, $n_f = 100$), and ($a = 3.5$, $n_f = 150$) the equivalent permeability is equal to $k_{\text{eq}} = 70.5$, 18.9, and $1.91 \times 10^{-15} \text{ m}^2$, respectively. The difference in the permeabilities between these cases at sufficiently close densities $\gamma \in [0.05, 0.055]$ can reach 37 times. Therefore, in this case, it is not possible to construct a functional relationship between the density of the fracture system and the equivalent permeability of the medium. Thus, we can conclude that with the taken law of the fracture distribution over the lengths, the density of the system cannot unambiguously characterize the permeability of the fractured-porous medium.

Next, we will consider the dependence of k_{eq}/k_m on the percolation parameter p shown in Fig. 4. It can be seen that two sections with different character of the functional dependence $k_{\text{eq}}(p)$ can be distinguished on this dependence: up to the threshold value of the percolation parameter ($0 \leq p < p_c$) and thereafter ($p \geq p_c$). In the first section, at low values of the percolation parameter ($p < 1.7$), the value of the equivalent permeability of the medium is determined by the matrix permeability: in this area, the fractures are isolated from each other by the rock matrix. Then, as p increases and approaches the percolation threshold, an increase in the permeability is observed. This is caused by increase in the degree of connectivity of the fracture system. In the second section, a developed system of fractures forms a percolation cluster, which has a decisive influence on the fluid flow. In this case, the Fractures act as “main channels” for flows through the porous medium. In this case, the greatest uncertainty in the equivalent permeabilities takes place in the “transition zone” ($1.7 < p < 7.9$).

Taking into account the above, the approximation of the equivalent permeability $k_{\text{eq}}(p)$ was carried out using a given continuous piecewise function that takes into account the features of the fracture system structure. At $p \leq p_c$, the equivalent permeability is approximated using the weighted harmonic mean determined by formula (4.3), where the value of $p/p_c \in [0; 1]$ is used instead of fraction of the computational area occupied by fractures l_{\parallel}/L . The power-law nature of the dependence of the equivalent permeability on the percolation parameter proposed in [34] was also taken into account. In addition, the approximating function must satisfy the following conditions: $k_{\text{eq}} = k_m$ at $p = 0$ and $k_{\text{eq}} = k_c$ at $p = p_c$, where k_c is the permeability of a fractured-porous medium at the percolation threshold. Thus, to approximate the equivalent permeability of a fractured-porous medium at $p \leq p_c$, the following function can be used:

$$k_{\text{eq}} = \left(\frac{p_c (k_m)^{1/\alpha} (k_c)^{1/\alpha}}{p (k_m)^{1/\alpha} + (p_c - p) (k_c)^{1/\alpha}} \right)^{\alpha}. \quad (4.4)$$

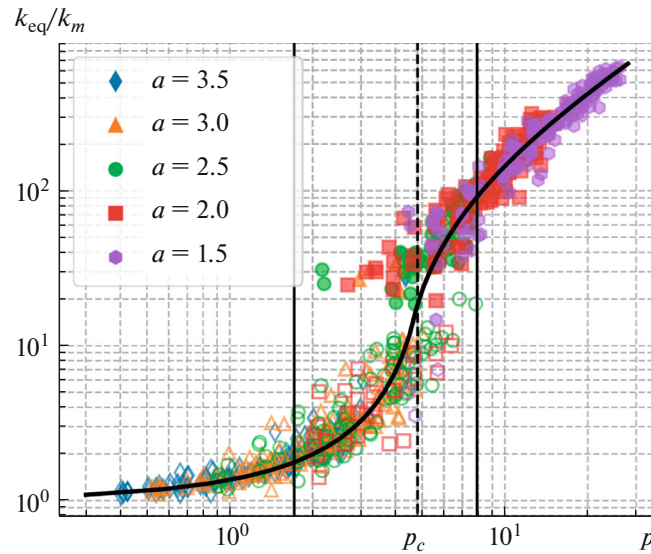


Fig. 4. Ratio k_{eq}/k_m as a function of the percolation parameter p for various power law exponents a and its approximation. Filled markers correspond to the case of percolation of the computational domain and hollow markers correspond to the absence of a percolation cluster.

It is known that the behavior of the permeability of a system of fractures above the percolation threshold has a power-law character [35, 36]. Therefore, at $p \geq p_c$, the following power function can be used:

$$k_{eq} = k_c (p - p_c + 1)^\beta, \tag{4.5}$$

where $k_{eq} = k_c$ at $p = p_c$.

Thus, expressions (4.4) and (4.5) define a continuous piecewise function with adjustable parameters: α, k_c, β . The result of the approximation of the results of numerical simulation is shown in Fig. 4. For the quality control of the approximation, the mean absolute percentage error $mape = \frac{1}{n} \sum_{i=1}^n \frac{|\hat{y}_i - y_i|}{|y_i|} = 0.2$ is used. The obtained quality of the approximation is satisfactory under the conditions that in the transition zone the equivalent permeabilities of the media at close values of the percolation parameter can differ by an order of magnitude.

As a result of the approximation for the parameters α and β , the values 1.6 and 1.11, respectively, are obtained. The value of β agrees well with the data given in the literature $\beta \approx 1.1$ [35]. To estimate the value of k_c , it should be noted that near the percolation threshold there is the only one way of connecting the opposite boundaries of the computational domain by fractures, which determines the hydraulic properties of the medium for $k_m \ll k_f$. Then the equivalent permeability near the percolation threshold k_c can be estimated from expression (4.2): $k_{||}^I = 26.6 \times 10^{-15} \text{ m}^2$ at $n_f = 1$. The value of $k_c = 18.8 \times 10^{-15} \text{ m}^2$ obtained by approximating the results of numerical simulation is somewhat lower than the analytical estimate, which can be explained by the tortuosity of the system of fractures connecting the opposite boundaries of the area. For example, in Fig. 1 ($a = 2.5, n_f = 100$) the shortest path along the fracture system between the left- and right-hand boundaries of the computational domain, which has a tortuosity, is marked by red curve.

In a particular case, as $k_m/k_c \rightarrow 0$, formula (4.4) can be reduced to the following form [34]:

$$k_{eq} = k_m \left(\frac{p_c}{p_c - p} \right)^\alpha.$$

Formula (4.4) also takes into account the limiting case of an impermeable rock matrix $k_m = 0$. In this case, the quantity $k_{eq} = 0$ at $p < p_c$ and jumps to k_c at $p = p_c$.

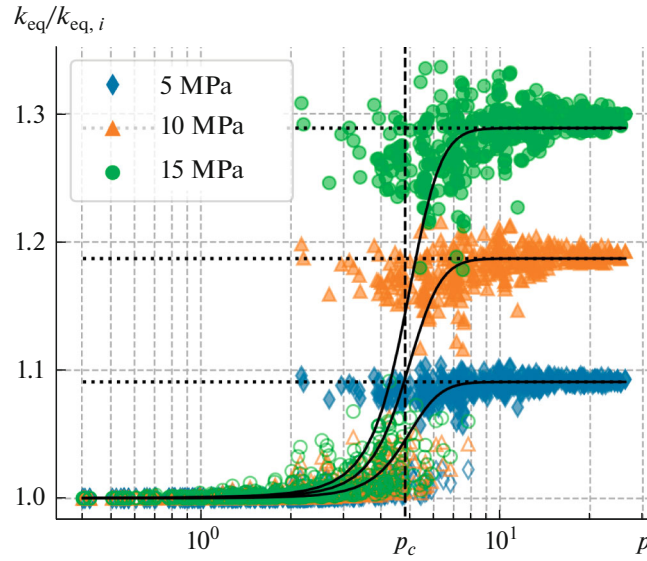


Fig. 5. Relative change in the equivalent permeability $k_{eq}/k_{eq,i}$ as a function of the percolation parameter p at various fluid injection pressures P_{in} . Filled markers correspond to the case of percolation of the computational domain and hollow markers correspond to the absence of a percolation cluster.

4.3. Effect of the Stress-Strain State

In this section, we study the variation in the equivalent permeability of a fractured-porous medium with change in its stress-strain state caused by fluid injection into the computational domain. The study was carried out at three values of fluid injection pressure $P_{in} = 5, 10, \text{ and } 15$ MPa and constant external loads $\sigma_b = 15$ MPa and pressures $P_{out} = 0$. The variation in the equivalent permeability is considered relative to its value $k_{eq,i}$, corresponding to the initial state of the medium, which has been studied in the previous paragraph.

In Fig. 5 we have plotted the graph of the relative variation in the equivalent permeability $k_{eq}/k_{eq,i}$ of the medium as a function of the percolation parameter p at various pressures P_{in} . It can be seen that the influence of the stress-strain state on the permeability of the medium increases with growth of the percolation parameter. Thus, at $p < p_c$, there is no significant effect of the injection pressure on the equivalent permeability of the medium. On the contrary, at $p > p_c$, the change in the fracture permeability begins to affect the hydraulic properties of the medium: the value of the relative variation in the equivalent permeability reaches 30%.

To select the approximating function, we will consider the effect of the stress-strain state on the permeability of a fractured medium consisting of a set of parallel fractures at $l_{\parallel} \geq L$. For simplicity of the estimates obtained below, in (4.2) we will neglect the permeability of the rock matrix as compared to the fracture permeability. Then, taking into account the dependence of the fracture aperture on the effective stresses (1.3), the expression for the permeability of a system of parallel fractures can be written as follows:

$$k_{\parallel}^I = \frac{\left(\delta_0 + \frac{\sigma'_n}{k_n}\right)^3}{12} \frac{n_f}{L}.$$

In this case, the expression for the relative change in the permeability of a set of parallel fractures with variation in the normal effective stresses takes the form:

$$\frac{k_{\parallel}^I}{k_{\parallel,i}^I} = \left(\frac{\delta_0 k_n + \sigma'_{ni} + \Delta\sigma'_n}{\delta_0 k_n + \sigma'_{ni}}\right)^3 = \left(1 + \frac{\Delta\sigma'}{\delta_0 k_n + \sigma'_{ni}}\right)^3 = (1 + b\Delta\sigma'_n)^3, \quad (4.6)$$

where $k_{||i}$ is the permeability of an ordered system of fractures under the initial conditions, $\Delta\sigma'_n$ is the change in the effective normal stresses relative to the initial state, $b = \frac{1}{\delta_0 k_n + \sigma'_{ni}}$ is a parameter of the fractured medium that depends on the initial stress-strain state of the medium and the elastic properties of fractures, and $\delta_0 k_n$ is the quantity corresponding to the fracture closure stress at a constant fracture stiffness.

In Fig. 5 the values of $k_{||}^I/k_{||i}^I$ are plotted for various injection pressures P_{in} in form of horizontal dotted lines. In place of $\Delta\sigma'_n$, in formula (4.6) we have used the following estimate of the change in the average effective stress in the computational domain $\Delta\sigma'_n = \sigma_b + b_f \left(\frac{P_{in} + P_{out}}{2} - P_i \right)$. It can be seen that at $p > 7.9$ the resulting estimate has a satisfactory approximation to the results of direct numerical simulation. Expression (4.6) is taken as the value of the maximum relative permeability change $k_{eq}/k_{eq,i}$. On the other hand, the permeability of the medium is equal to $k_{eq} = k_{eq,i}$ at $p = 0$. To plot the dependence of the equivalent permeability on p over the entire range of values, we have used an approximation of the percolation probability of the computational domain $S(p)$, which links the domains $p < 1.7$ and $p > 7.9$. Then, taking into account the change in its stress-strain state, the approximation of the equivalent permeability of the medium, can finally be represented in the form:

$$k_{eq} = [(1 + b\Delta\sigma'_n)^3 - 1]S(p) + 1]k_{eq,i}. \tag{4.7}$$

In Fig. 5 we have reproduced the result of the approximation of changes in the equivalent permeability by the function (4.7). A satisfactory quality of approximation was obtained, the mean absolute percentage error for various fluid injection pressures took the following values: $mape = 0.007$ at $P_{in} = 5$ MPa, $mape = 0.015$ at $P_{in} = 10$ MPa, and $mape = 0.023$ at $P_{in} = 15$ MPa.

Thus, the proposed approximation (4.7) takes into account the dependence of the equivalent permeability of the fractured-porous medium on all the main parameters of the problem: the structure of the fracture system (the percolation parameter p and its threshold value p_c), the stress-strain state of the system (the values of the effective stresses σ'_n), and the fractures properties (normal stiffness k_n and fracture aperture δ).

SUMMARY

The study of the dependence of the equivalent permeability of fractured-porous media on their stress-strain state and the structure of the system of fractures was carried out. To simulate the flow through the deformable fractured-porous medium, a model of a poroelastic medium was used. Fracture network was simulated using the discrete fracture model. The fracture length distribution follows the power law. The numerical study was carried out for different realization of the fracture systems obtained by multiple random generation.

The results obtained show that the permeability of a fractured-porous medium is determined mainly by the structure of the fracture system characterized by the percolation parameter. In this case, near the percolation threshold, there is a change in the behavior of the equivalent permeability and its sharp increase. At the same time, the density of the fracture network does not allow to describe the equivalent permeability of the medium with satisfactory accuracy.

It is shown that the hydraulic properties are significantly affected by the stress-strain state only for strongly connected fractured systems with the percolation parameter $p > 7.9$. According to the simulations results, for the performed calculations the change in the equivalent permeability reached 30%. For weakly connected fracture systems ($p < 1.7$), the maximum relative change in the permeability is less than 1%.

An approximating equation is proposed to define the dependence of the equivalent permeability of a fractured-porous medium on the following parameters: the connectivity of the fracture system, the stress-strain state of the medium, and the fracture characteristics such as the stiffness and the aperture.

FUNDING

The work was carried out within the state assignment of Ministry of Science and Higher Education of the Russian Federation (project no. 121030500156-6).

REFERENCES

1. Smirnov, N.N., Nikitin, V.F., Kolenkina (Skryleva), E.I., and Gazizova, D. R., Evolution of a phase interface in the displacement of viscous fluids from a porous medium, *Fluid Dyn.*, 2021, vol. 56, no. 1, pp. 79–92. <https://doi.org/10.1134/S0015462821010122>
2. Nikitin, V.F., Skryleva, E.I., and Weisman, Yu.G., Control of capillary driven fluid flows for safe operation of spacecraft fluid supply systems using artificial porous media, *Acta Astronautica.*, 2022, vol. 194, pp. 544–548. <https://doi.org/10.1016/j.actaastro.2021.12.009>
3. Dushin, V.R., Smirnov, N.N., Nikitin, V.F., Skryleva, E. I., and Weisman, Yu.G., Multiple capillary-driven imbibition of a porous medium under microgravity conditions: Experimental investigation and mathematical modeling, *Acta Astronautica*, 2022, vol. 193, pp. 572–578, <https://doi.org/10.1016/j.actaastro.2021.06.054>
4. Kiselev, A.B., Kay-Zhui, L., Smirnov, N.N., and Pestov, D.A., Simulation of fluid flow through a hydraulic fracture of a heterogeneous fracture-tough reservoir in the planar 3D formulation, *Fluid Dyn.*, 2021, vol. 56, no. 2, pp. 164–177. <https://doi.org/10.1134/S0015462821020051>
5. Smirnov, N., Li, K., Skryleva, E., Pestov, D., Shamina, A., Qi, C., and Kiselev, A., Mathematical modeling of hydraulic fracture formation and cleaning processes, *Energies*, 2022, vol. 15, no. 6. <https://doi.org/10.3390/en15061967>
6. Van Golf-Racht, T.D., *Fundamentals of Fractured Reservoir Engineering*, Amsterdam: Elsevier, 1982.
7. Nelson, R.A., *Geologic Analysis of Naturally Fractured Reservoirs*, Gulf Professional Publishing, 2001.
8. Pichugin, O.N., Rodionov, S.P., Solyanoi, P.N., Gavris', A.S., Kosyakov, V.P., and Kosheverov, G.G., Principles of optimization of the oilfield flooding systems for oilfields complicated with low-amplitude tectonic violations, in: *SPE Russian Oil and Gas Technological Conference*, Moscow, Russia, 2015. <https://doi.org/10.2118/176697-MS>
9. Karimi-Fard, M., Durlofsky, L.J., and Aziz, K., An efficient discrete-fracture model applicable for general-purpose reservoir simulators, *SPE J.*, 2004, vol. 9, no. 2, pp. 227–236. <https://doi.org/10.2118/88812-PA>
10. Garipov, T.T., Karimi-Fard, M., and Tchelepi, H.A., Discrete fracture model for coupled flow and geomechanics, *Comput. Geosci.*, 2016, vol. 20, no. 1, pp. 149–160. <https://doi.org/10.1007/s10596-015-9554-z>
11. Bai, M., On equivalence of dual-porosity poroelastic parameters, *J. Geophys. Res: Solid Earth*, 1999, vol. 104, no. B5, pp. 10461–10466. <https://doi.org/10.1029/1999JB900072>
12. Chen, H.-Y. and Teufel, L.W. Coupling fluid-flow and geomechanics in dual-porosity modeling of naturally fractured reservoirs—model description and comparison, in: *SPE Int. Oil Conf. and Exh. in Mexico, 2000*. <https://doi.org/10.2118/59043-MS>
13. Rutqvist, J. and Stephansson, O., The role of hydromechanical coupling in fractured rock engineering, *Hydrogeol. J.* 2003, vol. 11, no. 1, pp. 7–40. <https://doi.org/10.1007/s10040-002-0241-5>
14. Biot, M.A., General theory of three-dimensional consolidation, *J. Appl. Phys.*, 1941, vol. 12, no. 2, pp. 155–164. <https://doi.org/10.1063/1.1712886>
15. Coussy, O., *Poromechanics*, Wiley, 2004.
16. Gutierrez, M. and Youn, D.-J., Effects of fracture distribution and length scale on the equivalent continuum elastic compliance of fractured rock masses, *J. Rock Mech. Geotech. Eng.*, 2015, vol. 7, no. 6, pp. 626–637. <https://doi.org/10.1016/j.jrmge.2015.07.006>
17. Liu, R., Li, B., Jiang, Y., and Huang, N., Review: Mathematical expressions for estimating equivalent permeability of rock fracture networks, *Hydrogeol. J.*, 2016, vol. 24, no.7, pp. 1623–1649. <https://doi.org/10.1007/s10040-016-1441-8>
18. Bonnet, E., Bour, O., Odling, N.E., Davy, P., Main, I., Cowie, P., and Berkowitz B., Scaling of fracture systems in geological media, *Rev. Geophys.*, 2001, vol. 39, no. 3, pp. 347–383. <https://doi.org/10.1029/1999RG000074>
19. Bogdanov, I.I., Mourzenko, V.V., Thovert, J.-F., and Adler, P.M., Effective permeability of fractured porous media in steady state flow, *Water Resour. Res.*, 2003, vol. 39, no. 1. <https://doi.org/10.1029/2001WR000756>
20. Hyman, J.D., Karra, S., Carey, J.W., Gable, C.W., Viswanathan, H., Rougier, E., and Lei, Z., Discontinuities in effective permeability due to fracture percolation, *Mech. Mater.*, 2018, vol. 119, pp. 25–33. <https://doi.org/10.1016/j.mechmat.2018.01.005>
21. Jafari, A. and Babadagli, T., A sensitivity analysis for effective parameters on 2D fracture-network permeability, *SPE Res. Eval. Eng.*, 2009, vol. 12, no. 3, pp. 455–469. <https://doi.org/10.2118/113618-PA>

22. Bour, O. and Davy, P., Connectivity of random fault networks following a power law fault length distribution, *Water Resour. Res.*, 1997, vol. 33, no. 7, pp. 1567–1583.
<https://doi.org/10.1029/96WR00433>
23. de Dreuzy, J.-R., Davy, P., and Bour, O., Hydraulic properties of two-dimensional random fracture networks following a power law length distribution: 1. Effective connectivity, *Water Resour. Res.*, 2001, vol. 37, no. 8, pp. 2065–2078.
<https://doi.org/10.1029/2001WR900011>
24. de Dreuzy, J.-R., Davy, P., and Bour, O., Hydraulic properties of two-dimensional random fracture networks following a power law length distribution: 2. Permeability of networks based on lognormal distribution of apertures, *Water Resour. Res.*, 2001, vol. 37, no. 8, pp. 2079–2095.
<https://doi.org/10.1029/2001WR900010>
25. Masihi, M. and King, P.R., Connectivity prediction in fractured reservoirs with variable fracture size: Analysis and validation, *SPE J.*, 2008, vol. 13, no. 1, pp. 88–98.
<https://doi.org/10.2118/100229-PA>
26. Witherspoon, P.A., Wang, J.S.Y., Iwai, K., and Gale, J.E., Validity of cubic law for fluid flow in a deformable rock fracture, *Water Resour. Res.*, 1980, vol. 16, no. 6, pp. 1016–1024.
<https://doi.org/10.1029/WR016i006p01016>
27. Gao, K. and Lei, Q., Influence of boundary constraints on stress heterogeneity modelling, *Comput. Geotech.*, 2018, vol. 99, pp. 130–136.
<https://doi.org/10.1016/j.compgeo.2018.03.003>
28. Tang, T., Hededal, O., and Cardiff, P., On finite volume method implementation of poro-elasto-plasticity soil model, *Int. J. Numer. Anal. Meth. in Geomech.*, 2015, vol. 39, no. 13, pp. 1410–1430.
<https://doi.org/10.1002/nag.2361>
29. Kim, J., Tchelepi, H.A., and Juanes, R., Stability and convergence of sequential methods for coupled flow and geomechanics: Fixed-stress and fixed-strain splits, *Comp. Meth. Appl. Mech. Eng.*, 2015, vol. 200, no. 13, pp. 1591–1606.
<https://doi.org/10.1016/j.cma.2010.12.022>
30. Geuzaine, C. and Remacle, J.-F., Gmsh: A 3-D finite element mesh generator with built-in pre- and post-processing facilities, *Int. J. Num. Meth. Eng.*, 2009, vol. 79, no. 11, pp. 1309–1331.
<https://doi.org/10.1002/nme.2579>
31. Legostaev, D.Y. and Rodionov, S.P. Numerical study of a two-phase fluid flow in a fractured porous medium based on models of poroelasticity and discrete fractures. *J. Appl. Mech. Tech. Phys.*, 2021, vol. 62, no. 3, pp. 458–466.
<https://doi.org/10.1134/S0021894421030123>
32. Berre, I., Doster, F., and Keilegavlen, E., Flow in fractured porous media: A review of conceptual models and discretization approaches, *Transp. in Porous Media*, 2019, vol. 130, no. 1, pp. 215–236.
<https://doi.org/10.1007/s11242-018-1171-6>
33. Basniev, K.S., Kochina, I.N., and Maksimov, B.M., *Podzemnaya gidromekhanika* (Underground Hydromechanics), Moscow: Nedra, 1993.
34. Lei, Q., Wang, X., Min, K.-B., and Rutqvist, J., Interactive roles of geometrical distribution and geomechanical deformation of fracture networks in fluid flow through fractured geological media, *J. Rock Mech. Geotech. Eng.*, 2020, vol. 12, no. 4, pp. 780–792.
<https://doi.org/10.1016/j.jrmge.2019.12.014>
35. Hestir, K. and Long, J.C.S., Analytical expressions for the permeability of random two-dimensional Poisson fracture networks based on regular lattice percolation and equivalent media theories, *J. Geophys. Res: Solid Earth.*, 1990, vol. 95, no. B13, pp. 21565–21581.
<https://doi.org/10.1029/JB095iB13p21565>
36. Berkowitz, B. and Balberg, I., Percolation theory and its application to groundwater hydrology, *Water Resour. Res.*, 1993, vol. 29, no. 4, pp. 775–794.
<https://doi.org/10.1029/92WR02707>

Translated by E.A. Pushkar